Advanced Review

Climate trends in the Arctic as observed from space

Josefino C. Comiso* and Dorothy K. Hall

The Arctic is a region in transformation. Warming in the region has been amplified, as expected from ice-albedo feedback effects, with the rate of warming observed to be ~0.60 ± 0.07°C/decade in the Arctic (>64°N) compared to ~0.17°C/decade globally during the last three decades. This increase in surface temperature is manifested in all components of the cryosphere. In particular, the sea ice extent has been declining at the rate of ~3.8%/decade, whereas the perennial ice (represented by summer ice minimum) is declining at a much greater rate of ~11.5%/decade. Spring snow cover has also been observed to be declining by −2.12%/decade for the period 1967–2012. The Greenland ice sheet has been losing mass at the rate of ~34.0 Gt/year (sea level equivalence of 0.09 mm/year) during the period from 1992 to 2011, but for the period 2002–2011, a higher rate of mass loss of ~215 Gt/year has been observed. Also, the mass of glaciers worldwide declined at the rate of 226 Gt/year from 1971 to 2009 and 275 Gt/year from 1993 to 2009. Increases in permafrost temperature have also been measured in many parts of the Northern Hemisphere while a thickening of the active layer that overlies permafrost and a thinning of seasonally frozen ground has also been reported. To gain insight into these changes, comparative analysis with trends in clouds, albedo, and the Arctic Oscillation is also presented.

How to cite this article:
WIREs Clim Change 2014, 5:389–409. doi: 10.1002/wcc.277

INTRODUCTION

The Arctic is an area of intense interest because climate-change signals are expected to be amplified in the region by about 1.5–4.5 times.[1] Ice-albedo feedback effect[1,2] associated with the high albedo of snow and ice which cover a large fraction of the region has been postulated as one of the key reasons for the amplification of the warming. As the snow and ice retreat, more heat is absorbed by the Earth's surface causing a warmer surface that in turn causes more melt and enhanced retreat of the snow/ice. The Arctic is also vulnerable to rapid changes because snow and ice are very sensitive to increases in surface temperature especially near melt temperatures.

In recent decades, the Arctic has indeed undergone considerable change. The sea ice and snow cover and the mountain glaciers in the Northern Hemisphere (NH) are declining and retreating, the ice sheet in Greenland has been losing mass and the permafrost in parts of North America and Eurasia has been increasing in temperature, and even thawing in some areas. These phenomena have been reported in a vast number of publications in recent years.[3–8] Attribution studies have been conducted using numerical modeling but results have not been consistent and more research is needed to explain the character and the magnitude of the trends. The purpose of this article is to provide an overview of the changes in the Arctic climate as reflected in its major components and as inferred primarily from satellite data.

*Correspondence to: josefino.c.comiso@nasa.gov

Cryospheric Sciences Laboratory, Code 615 Earth Sciences Division, NASA Goddard Space Flight Center, Greenbelt, MD, USA

Conflict of interest: The authors have declared no conflicts of interest for this article.

THE ARCTIC ENVIRONMENT AND MEASUREMENT CHALLENGES

The Arctic consists of the Arctic Ocean, the peripheral seas, the northern parts of North America (including Greenland) and Eurasia. The central region is covered mainly by sea ice and open water that is surrounded by land that is underlain by permafrost and at least partly covered by snow, glaciers, ice caps, and the Greenland ice sheet. The southern boundary of the Arctic has been loosely defined by some as the Arctic Circle (66° 33′N)—the approximate location of the edge of the midnight sun and polar night. We use in our study an extended boundary since trends in the Arctic can be evaluated more effectively by examining the changes in the various components of the cryosphere some of which are in areas found south of the Arctic Circle. The location map in Figure 1 shows the distribution of sea ice during the end of summer in 2012, the typical location of the end of summer ice edge (yellow line) and the locations or boundaries of glaciers, ice sheet, snow, and permafrost in land areas. The sea ice cover extends into the sub-Arctic and as far south as 44°N in the peripheral seas during winter. Permafrost, snow cover, and the Greenland ice sheet all extend south of the Arctic Circle.

Adverse weather conditions, extremely cold temperatures especially in winter, thick and almost impenetrable sea ice cover, and prevailing darkness in winter are among the many challenges of making measurements in the Arctic. Logistical problems are further confounded by the challenge of designing instruments that can provide accurate measurements consistently under extreme conditions and maintaining these instruments so they continue to provide reliable and consistent information. Transport of equipment can also be a problem because of inability of most ships to navigate through sea ice and the difficulty of snow machines to get through barriers like ridges and leads in sea ice. Over ice masses and glaciers, the rugged terrain and the presence of crevasses also pose problems. Additionally, working in mountain snow covers can be hazardous due to avalanches and difficulties in traveling through deep snow. Although the recent warming of the Arctic and the rapid retreat of perennial ice has led to the opening of the Northeast and Northwest passages in some summers and made logistics in the region somewhat less difficult, measurement challenges persist.

The use of satellite data has revolutionized our ability to study the Arctic. The data have led to the discovery of many unexpected phenomena and events in both polar regions. However, many measurement challenges remain. Satellite-borne passive microwave systems have provided continuous coverage of the sea ice cover for more than four decades and have revealed details on the large-scale distribution of the sea ice cover at a good temporal resolution, though, the spatial resolution is only about 12–25 km which is good enough for most large-scale studies, but a full characterization of some of important processes like polynya formation, Polar Lows and divergence that takes place inside the ice pack is not possible. Additionally, the retrieval of some parameters, like temperature, albedo and cloud cover, is oftentimes compromised because of persistent cloud cover in the Arctic and the difficulty of accurately discriminating clouds from snow and ice. Optimal cloud masks have been elusive but the advent of new sensors has led to considerable improvements in this regard. Despite the many challenges, however, satellite data provide a consistent, accurate, and comprehensive record suitable for climate-change trend studies.

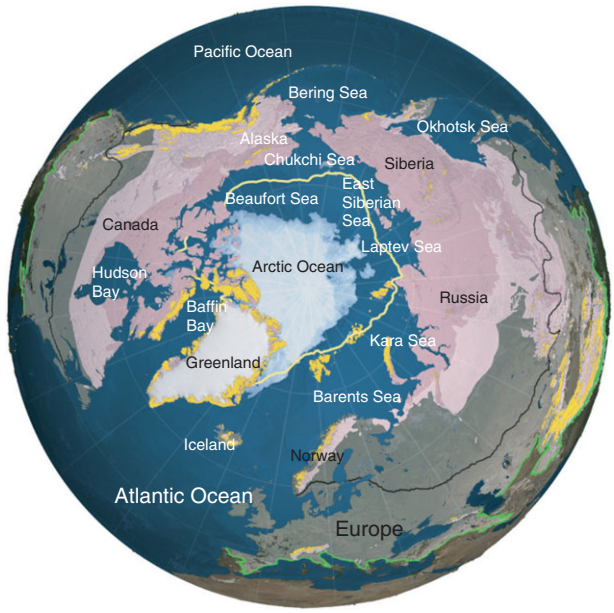

FIGURE 1 | Location map of the Arctic region including average sea ice extent (yellow line), sea ice cover during record minimum in summer of 2012 (shades of white), continuous and discontinuous permafrost (shades of pink), glacier locations (gold dots), and snow-cover (average location of 50% snow line in black and maximum snow line in green as inferred from moderate-resolution imaging spectroradiometer (MODIS) data).

OBSERVED CHANGES IN THE ARCTIC

Variability and Trends in Surface Temperature

Surface temperature is one of the key parameters that determines the state of the Arctic. More specifically, it is temperature that determines the thermodynamic

state of the various surfaces, especially those that are ice covered. For example, the length of subfreezing (or melt) temperatures determines the extent, thickness and duration of many cryospheric parameters. In conjunction with surface albedo, temperature controls the amount of energy transferred between the ocean and the atmosphere, including turbulent, sensible, and latent heat fluxes.

Using data from meteorological stations worldwide along with other sources of *in situ* data, global temperatures have been shown to have increased by about 0.8°C since 1900.[9–12] A general warming in the Arctic using the limited and spatially sparse *in situ* data has also been reported.[13] Warming was also reported using a pan-Arctic data set that was created by filling in the gaps of *in situ* and buoy temperature data through the use of a sophisticated spatial interpolation technique.[14] Reanalysis data from ERA-40 and national center for environmental prediction (NCEP) data have also been used for temperature change studies[15] but the accuracy depends on the availability of *in situ* data which are sparse in the region and may not be as reliable for trend studies as those derived from satellite data.[16]

Monthly averages of surface temperature in the Arctic region, as derived from the advanced very high resolution radiometer (AVHRR), have been compiled and analyzed for the period August 1981 through the most recent data available using different algorithms.[16,17] The results from different sources provide similar patterns of temperature distribution but yield significantly different variability and trends not only because of differences in techniques but also in resolving differences in the calibration of the different AVHRR sensors and in addressing atmospheric corrections.[16]

Improved surface temperature maps of Greenland using moderate-resolution imaging spectroradiometer (MODIS) data have been generated[18] but the record length of MODIS (2000–2014) is currently too short for meaningful trend analysis. However, during this period some unexpected events were observed including the occurrence of unusually extensive surface melt events in 2002 and 2012.[19,20] The historical surface temperature satellite data show large seasonality of surface temperature with the monthly averages ranging from −29°C to 0°C inside the Arctic Circle.[21] The coldest regions in the Arctic are most consistently located at the high elevations of the Greenland ice sheet but there are times when surface temperatures in parts of Siberia are even colder.

To gain insight into how surface temperatures have been changing in various parts of the Arctic a color-coded map of trends in surface temperature using the 1981–2012 monthly anomaly data is presented in Figure 2(a). The monthly anomaly data which have been updated from a previous version[16] were derived using satellite climatology as the baseline. Although the trends are spatially variable, they are mainly positive. Unusually high positive values are shown over sea ice but these are mainly in areas where the summer ice edges have been retreating in recent years. There are also some negative trends, predominantly located in parts of Siberia and in the Bering Sea, that are associated primarily with unusually warm conditions in the region in the 1980s.

Using the updated version of the Goddard institute for space studies (GISS) data set,[9] the trend in global temperature has been estimated to be about 0.081°C/decade (very likely between 0.074 and 0.088°C/decade) for the period from 1900 to 2012. The 'very likely' range in trend corresponds to 90% confidence level. For the period 1981–2012, the trend in surface temperature using GISS data,[9] was estimated, as shown in Figure 2(b), to be 0.17°C/decade (very likely between 0.14 and 0.20) for the entire globe and 0.60°C/decade (very likely between 0.48 and 0.71°C/decade) for the Arctic region (>64°C). These results represent an acceleration of the global trend and an amplification by more than three times in the Arctic region showing consistency with modeling predictions. For comparison, the corresponding trend in temperature using AVHRR data for the same time period in the Arctic (>64°C) is 0.69°C/decade (very likely between 0.56 and 0.82°C/decade). The slightly greater trend in Arctic temperatures from AVHRR is mainly due to stronger trends in the Central Arctic Basin (see Figure 2(a)) where *in situ* data are very sparse.[16] These results indicate a general consistency of *in situ*/station temperature data with satellite data. The trend results are slightly different but consistent with those reported previously but using a different algorithm for temperature and a shorter time period.[18] The errors quoted are for statistical errors of the trends and do not include systematic errors which are unknown but expected to change only slightly from one year to another and would not significantly affect the errors in the trends. The range of values with 90% confidence level and referred to as the very likely range is also provided.

To illustrate how the temperature varied on a monthly basis from one region to another, monthly temperature anomalies over four key regions (namely: sea ice, Greenland, Eurasia, and North America) were calculated and the results together with 12-month running averages (in red), are presented in Figures 2(c)–(f). The plots indicate that there were years when it was unusually warm (e.g., 1995)

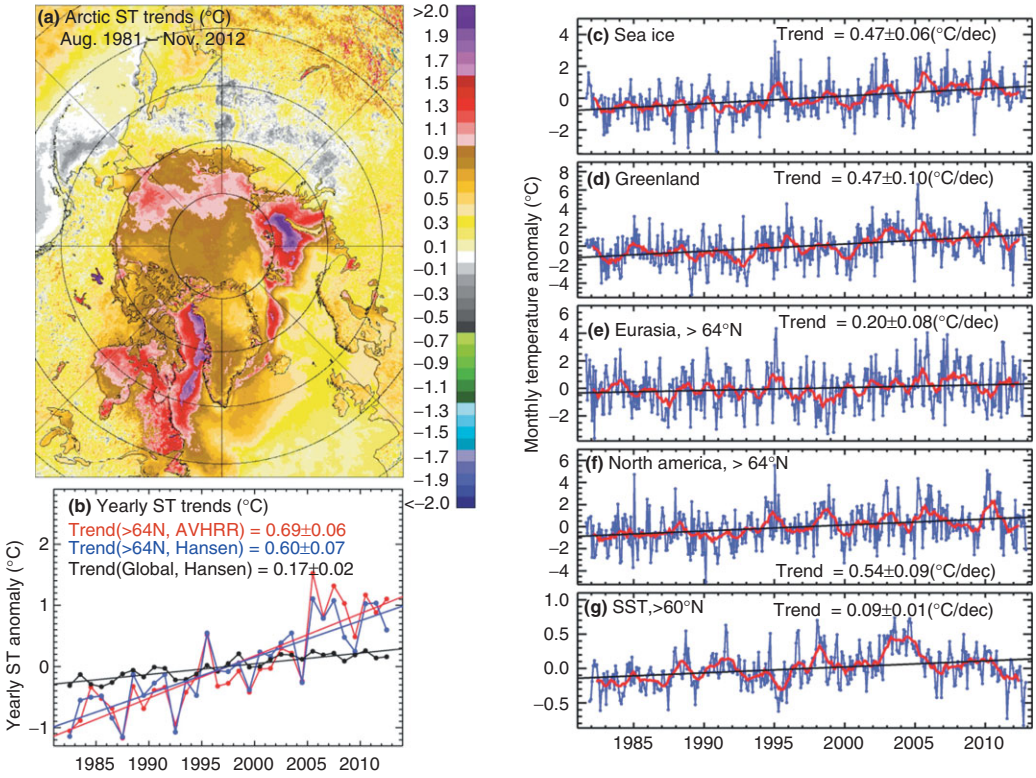

FIGURE 2 | (a) Color-coded surface temperature trends for the entire Arctic using August 1981–November 2012 advanced very high resolution radiometer (AVHRR) data; (b) plots of yearly anomalies and trends for the entire globe (black) and for the Arctic region (>64°N) using Hansen (2010) (blue) and AVHRR (red) data; and plots of anomalies (blue), 1-year running average (red) and linear trend (black) for (c) sea ice; (d) Greenland; (e) Eurasia, >64°N; (f) North America, >64°N; and (g) SST, >60°N.

and years when it was unusually cold (e.g., 1982). The trend in temperature over sea ice covered regions is estimated to be 0.47°C/decade (very likely between 0.37 and 0.57°C/decade at 90% confidence level), whereas the trend was significantly higher at 0.77°C/decade (very likely between 0.60 and 0.94°C/decade) over Greenland. The high trend values in Figure 2(a) are over the sea ice regions that are located in areas where sea ice had been displaced by open water in later years during the ice melt season. In the region >64°N, the trend is 0.20°C/decade (very likely between 0.07 and 0.33°C/decade in Eurasia) which is low compared to 0.54°C/decade (very likely between 0.34 and 0.69) for North America because of the negative trends in Siberia as shown in Figure 2(a). Again, the errors quoted are the statistical errors and there is a 90% confidence level that the trends are within the range indicated.

Changes in the ocean temperature in the Arctic region have been reported in several studies.[22,23] The temperature of the mixed layer has apparently been affected by ice-albedo feedback on account of recent declines in the summer ice cover and increases in dynamics both for the ice cover and the underlying ocean. The mixed layer temperature has recently been affected by changes in the extent and frequency of leads in autumn and winter as may be caused by changes in atmospheric circulation.[23] The changes are monitored in part using satellite data which provide comprehensive coverage of sea-surface temperature (SST) in the region during clear-sky conditions[21] using AVHRR and MODIS data, and almost continuously using Scanning Multichannel Microwave Radiometer (SMMR), EOS/advanced microwave scanning radiometer (AMSR-E) and AMSR2 data.[23–25] Using AVHRR data, the monthly anomalies of SST are presented in Figure 2(g) for >60 N and regression analysis yielded a trend of 0.04°C/decade (very likely between 0.02 and 0.06°C/decade). The trend is modest but using AMSR-E data, SST has been shown to increase rapidly (5°C over a 7-day period) to an unusually high value in the western region in 2007,[23] when a dramatic decline in the sea ice cover was observed, as discussed in the next section.

Variability and Trends in the Sea Ice Cover

The Arctic sea ice cover is part of the polar heat sink and is considered a key component of the

climate system. It has seasonal ice and perennial ice components with each component representing approximately half (about 8×10^6 km^2) of the maximum extent during the 1980s when the passive microwave satellite series just began.[26] The perennial ice component is defined as the ice that survived at least one summer and is usually represented by the sea ice cover during ice minimum extent.[27] During the last three decades, the perennial component has been declining significantly while the total ice cover has also been decreasing but more modestly.[27,28] The net effect is an increasing extent of the seasonal sea ice cover.

Changes in the sea ice cover garnered significant attention when the perennial ice was first reported to be declining rapidly from the 1980s to the 1990s,[27] leading to concerns that in the foreseeable future, the Arctic Ocean would become a blue (ice free) ocean[29] in the summer. There was even greater concern when the Arctic ice cover was observed to be declining faster than what modeling studies had been predicting.[8] This means that there are some unexpected factors that caused the faster decline and that the models have to take into account the physics behind these factors. The concerns were exacerbated when the perennial ice extent went down drastically in 2007 and was reduced to 40% of the average extent of the perennial ice from 1979 to 2007.[30] This was followed by another decline to a new low in 2012, which has been attributed in part to the occurrence of a large though rare storm in August 2012.[31–33]

A key issue in the assessment of interannual variability and trends in the ice cover is the estimate of ice extent and ice area which are derived from sea ice concentrations retrieved from passive microwave data. Several algorithms have been developed to retrieve sea ice concentration.[34–37] There are significant differences in the ice concentration estimates[38] from the various techniques but comparative studies done in different institutions have led to the selection of two algorithms for generating the standard products used by the sea ice community. The two are the NASA Team algorithm (NT1) and the Bootstrap Algorithms with NT1 subsequently improved using a different technique called NT2.[39] A comparison of ice concentrations and trends from the Bootstrap and NT2 shows good consistency in derived concentrations and trends.[40] In this report, we use results from the Bootstrap algorithm because it is the one that can provide consistent data from 1978 to the present, as NT2 requires the use of 89 GHz data that was not available for most of the period from 1978 to 1992.

Averages of the sea ice concentrations during the first and second halves of the historical data set are presented in Figure 3(a) (1979–1995) and 3(b) (1996–2012), respectively, to illustrate typical sea ice distributions during the two periods and how they changed from one period to another. It is apparent that ice cover during the earlier period is significantly more extensive with higher concentration than that of the latter period, especially in the Arctic Basin. To quantify the difference in the distribution a difference map is presented in Figure 3(c). The difference map shows mainly negative values with the most negative located where the sea ice cover had been retreating most rapidly. There are a few areas where the difference is slightly positive (e.g., Bering Sea) but large negative values can be observed along the edges of the location of the summer ice cover. For comparison, the trends in ice concentration are estimated for each pixel and the results are depicted in Figure 3(d). As with the surface temperature trend in Figure 2, the trend map made use of monthly anomalies using as a baseline, climatologies derived from historical data from November 1978 to December 2012. The trend analysis assumes that the changes in ice concentration vary linearly with time for each data element which is not necessarily the case. It is apparent, that the trend and difference maps have very similar spatial distributions, but not always. Significant differences in the Okhotsk Sea, Chukchi Sea, and East Siberian Sea regions are apparent and are likely associated with the nonlinearity of the data used in the trend analysis in these regions.

A more quantitative representation of typical seasonal changes over different time periods is presented in Figure 3(e). Averages of ice extents for each day for the period 1979–1995 are depicted by the gray line while corresponding averages for the period 1996–2012 are represented by the black line. The gray and black lines show a considerable change in the seasonality of sea ice from the first period of satellite data to the second period, especially during the summer. The differences in average extents for the two periods are better quantified by the gold line (bottom line) which shows that the difference during the summer months (including September and October) is about twice as much as for the rest of the year. For comparison, daily values are presented for 2012 (green line) which is the year with record low perennial ice extent (Figure 1), for 2007 (blue line) which is the year with the second lowest perennial ice, and for 1980 (red line) which is when the perennial ice extent was highest during the satellite era. These three plots indicate large departures from the multiyear averages and illustrate how drastically the extent of the sea ice cover has changed since 1980.

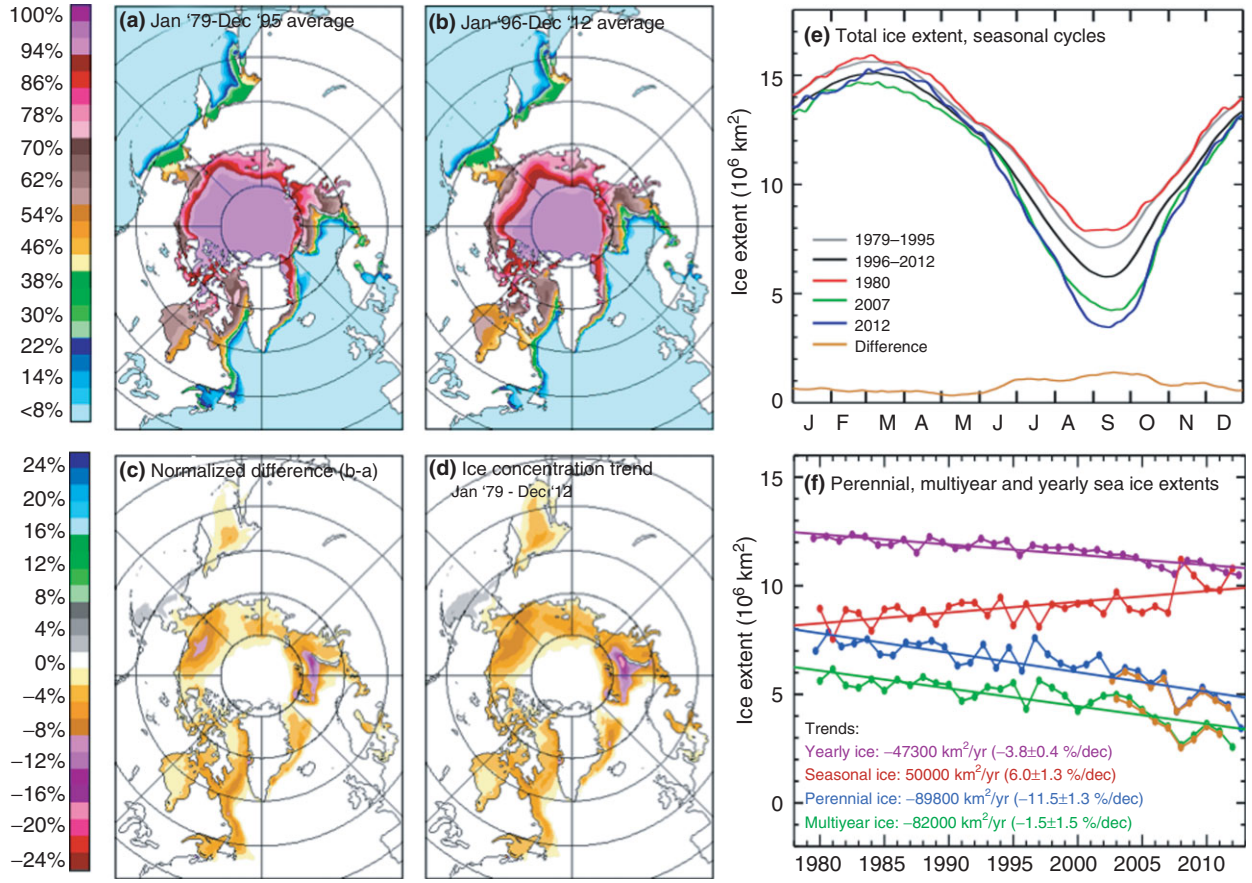

FIGURE 3 | (a) Color-coded average sea ice concentration map for (a) the period from January 1979 to December 1995; and (b) the period from January 1996 to December 2012. (c) Differences (for each pixel) of averages in (a) with averages in (b). (d) Trend map of sea ice concentration from January 1979 to December 2012. (e) Plots of daily averages of sea ice extent for the period 1979–1995 (in gray), sea ice extent from 1996 to 2012 (in black), difference of sea ice extent between the two periods (in gold, bottom plot); and daily sea ice extent for individual years in 1980 (when summer minimum was highest, in red), 2007 (when summer minimum was second lowest, in green) and 2012 (when summer minimum was a record low, in blue); (f) Ice extents and trends of yearly averages of sea ice extent (purple line), perennial ice (in blue), and multiyear ice (in green) for the 1979–2012 period using SMMR and SSM/I data. Also similar plots from AMSR-E data from 2003 to 2012 (gold) are presented for perennial and multiyear ice.

The changes in the entire Arctic ice cover are quantified in the set of plots presented in Figure 3. The yearly averages (Figure 3(a)) show significant interannual variability with a trend in ice extent of −473,000 km^2/decade or −3.8%/decade (very likely between −3.1 and −4.5%/decade). These values are generally consistent with those reported for a shorter period[28,41,42]but are significantly different for the percentage trends because a different baseline was used in the estimates. Our current values make use of the first data point (along the trend line) as the baseline instead of a climatological average. The first data point is regarded to yield a more accurate trend than the climatological average used in previous studies. For comparison, the trend in ice area was estimated to be −4.9%/decade (i.e., −526,000 km^2/decade) using the same data with the trend very likely between −4.6 and −5.2%/decade. The yearly extent of the perennial ice cover is also shown in Figure 3(f) (blue line) with the trend line indicating a rapid decline of −11.5%/decade (very likely between −9.3 and −13.7%/decade). Such rapid rate of decline indicates that the perennial ice, which is the mainstay of the Arctic ice cover and has been known to have existed for at least 1450 years,[43] is in the process of disappearing.[44] In addition, the multiyear ice (or ice that survives at least two summers) as derived from passive microwave data during the winter period,[45] is also declining even more rapidly at a rate of 13.5%/decade (with 90% confidence level that the trend is between −11.0 and −16.2%/decade). The AMSR-E data (in gold) provide an independent estimate of the perennial and multiyear ice extents and show good consistency with SSM/I data. Again, the values are slightly different from those quoted in the references because we now use a different but more accurate baseline.

The percentage trends are slightly less negative but the conclusions remain the same.

The net effect of a declining perennial and multiyear ice cover is a decline in average thickness which means that the volume of the ice is also declining. Direct measurements using available submarine, aircraft, and satellite data indeed indicate a considerable thinning of the sea ice cover. Thinning was reported using upward-looking sonar measurements of ice draft from submarines.[46,47] Ice, Cloud and Land Elevation Satellite (ICESat) data in combination with submarine data also show considerable change in ice thickness. In particular, measurements of ice keels from submarine upward-looking SONARs covering about 38% of the Arctic Ocean provided an average winter thickness of 3.64 m in 1980. By 2008, the average thickness over the same region has gone down to about 1.9 ± 0.5 m[48] (likely) indicating a 48% change in thickness. The impact is a more predominant seasonal (first year) sea ice cover which has been increasing at the rate of $6.0 \pm 1.3\%$ (likely)/decade from 1979 to 2012 (Figure 3(f)). This means more ice production in the Arctic Basin and therefore changes in the salinity and temperature structure for the Arctic Ocean. A thinner ice cover will also enhance ice drift velocities while more ice production will alter vertical as well as horizontal ocean circulation.

The variability of the Arctic sea ice cover over a time period extending before the satellite era is poorly known. A pan-Arctic data set on the sea ice cover for the period 1900–1979 has been put together using available data, climatology, and spatial interpolation.[49] Such data which have been updated using a more robust data set that starts in 1870 showed a fairly uniform distribution of the ice cover during the period with only a very slight negative trend. As *in situ* observations have been available, only in some regions of the Arctic the lack of variability is in part due to the extensive use of climatological data. Using terrestrial proxies from the circum-Arctic region, the decline of the summer sea ice cover in the last four decades has also been reported to be unprecedented for the past 1450 years.[43]

Trends in the NH Snow Cover

Snow cover is a sensitive indicator of climate change. It is also a powerful regulator of surface and near-surface air temperature because of its low thermal conductivity and high albedo. There is a strong positive feedback between snow cover (especially in the spring) and the radiation balance in the NH.[50] Snow-water equivalent (SWE), the quantity of water available when a snow cover melts, is a key snowpack parameter because as much as 80% of the water supply in some mountainous areas, such as the western United States, emanates from melting snow. Recent research suggests that snow cover and SWE in the NH has been decreasing, particularly in the springtime.[51]

Since 1966, data from geostationary operational environmental satellites (GOES), and from the very high resolution radiometer (VHRR) and its successor, the AVHRR, on polar orbiting environmental satellites (POES), have been used extensively by the National Oceanic and Atmospheric Administration (NOAA) to produce operational snow products.[52] In 1997, the Interactive Multisensor Snow and Ice Mapping System (IMS) (http://www.ssd.noaa.gov/PS/SNOW/ims.html) was developed to produce operational products daily at a spatial resolution of about 25 km, based on a variety of satellite data.[53,54] Subsequent improvements have increased the spatial resolution to 4 km. The Rutgers Global Snow Lab (GSL) reanalyzed snow cover between 1966 and 1971 using the same NOAA daily gridded composites of visible imagery for the eastern and western hemispheres of the NH used in the original mapping.[55] The Rutgers GSL dataset is now considered a climate-data record (CDR). With the advent of the MODIS, first launched on the Terra satellite in 1999, and later on the Aqua satellite in 2002, daily fractional snow-cover and snow-albedo maps have been available at a resolution of 500 m, thus permitting the most accurate fully automated daily global maps of snow cover to be produced routinely.[56,57]

Trend analysis results of the updated snow-cover extent (SCE) series have been used[58] to show that the NH spring snow cover has undergone significant reductions over the past 90 years and that the rate of decrease has accelerated over the past 40 years. In particular, the SCE has been reduced by 0.8×10^6 km^2/decade (7% in March and 11% in April and very likely between 4.5 and 9.5% in March and between 8.5 and 13.5% in April) for the period 1970–2010. Higher temperatures were determined to be the dominant factor in the observed SCE decreases, with air temperature anomalies over NH midlatitude land areas explaining 50% of the observed variability in SCE.[58] The uncertainty in the determination of SCE in NH spring has been estimated with 95% confidence level to be within the interval of ±5–10% over the pre-satellite period and ±3–5% over the satellite era.[58]

Spring (March, April, and May) snow-covered areas have been declining at a rate that is even greater than predicted by the Coupled Model Intercomparison Project Phase 5 (CMIP5) climate model

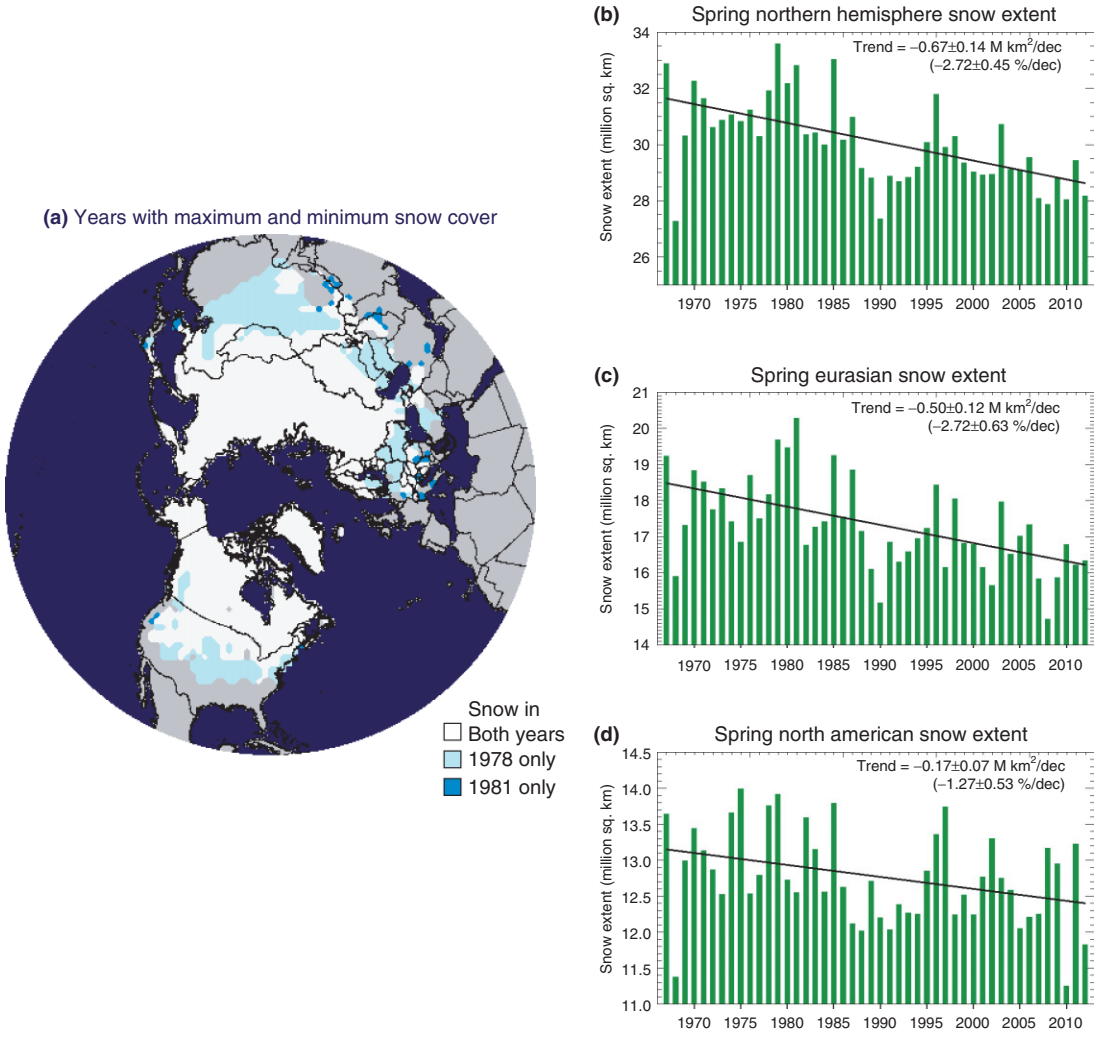

FIGURE 4 | (a) Years with maximum and minimum snow cover; data from the Rutgers University Global Snow Lab. Light blue represents snow cover in February of 1978 and dark blue represents snow cover in February of 1982 and white is snow in both years. (b) Northern Hemisphere snow cover in the spring, (c) Eurasian snow cover in the spring, and (d) North American snow cover in the spring, all showing declining trends in snow-cover extent during the satellite snow-mapping era.

simulations.[59] SCE results from the Rutgers GSL (http://climate.rutgers.edu/snowcover) for the period 1967–2012 are presented in Figure 4(a)–(d). The trend in earlier spring snowmelt in the NH (−2.12 ± 0.45%/decade), in particular, in Eurasia (−2.72 ± 0.63%/decade) since the beginning of the SCE record in the late 1960s is noted. The trend is more modest at −1.27 ± 0.53%/decade for the North American region.

From November to April, snow covers an average of about 33% of the land areas north of the Equator, and the maximum snow cover occupies about 49% of the land area in the month of January (see http://climate.rutgers.edu/snowcover and Ref 2). Warming has caused a trend toward earlier snowmelt in the Arctic, first noted in Refs 60 and 61 and later by many other researchers for the NH as a whole (e.g., Refs 51, 62–64).

Using a subset of the Rutgers ~47-year snow-cover CDR, a decrease in the duration of the NH snow season by 5.3 days/decade between the winters of 1972–1973 and 2007–2008 has been reported.[65] It was noted that the change is primarily a result of earlier snowmelt over western Europe, central and eastern Asia, and in the mountainous western United States. A key factor is the effect of surface air temperature anomalies that are known to control spring SCE.[66]

Use of the standard MODIS snow-cover products over 14 winters permits detailed regional monitoring of snow-covered mountains.[57,67–69] Using 40 years of stream discharge which provides indirect

snowmelt information and meteorological station data and 10 years of MODIS snow-cover products in the Wind River Range, Wyoming, USA, an earlier snowmelt in the decade of the 2000s as compared to the previous three decades was observed,[69] but no trend of earlier snowmelt *within* the decade of the 2000s was observed. The earlier snowmelt is likely due to documented increasing air temperatures during the 40-year period.

Other studies have shown that snowfall may be occurring later in the autumn in Eurasia in more recent years (versus earlier years in the ~47 year snow-cover CDR).[71] Thus, in many regions of the NH the snow-cover season is becoming shorter. The primary effect of the decreased duration of the snow season and the diminished snow extent during the spring months (Figure 4(a)–(c)) has been on the energy balance in late spring—reduced albedo due to earlier snowmelt and therefore greater absorption of energy at the surface.[51]

Mass Balance Studies of Small Glaciers and Ice Caps, and the Greenland Ice Sheet

Non-Ice Sheet Glaciers

The Earth's smaller glaciers and ice caps (non-ice sheet glaciers) cover an area of approximately 785,000 km^2 or a volume of ~250,000 km^3 which, if converted to meltwater, is equivalent to a rise in sea level of ~0.7 m.[72] This includes glaciers peripheral to the Greenland and Antarctic ice sheets. The current contribution to sea level from the Earth's smaller glaciers is ~1 mm/year, but the loss of glacier ice to the oceans is accelerating.[72] Through modeling, estimates show that the largest future contributions of smaller glaciers to sea level rise will be from glaciers in Arctic Canada, Alaska, and Antarctica.[73] There has also been dramatic glacier recession in the European Alps.[74]

The Global Land Ice Measurements from Space (GLIMS) project follows the Satellite Image Atlas of Glaciers of the World multi-decade and multinational project led by Richard S. Williams who is now an Emeritus Scientist at the U.S. Geological Survey (USGS). There are 11 'Atlas' volumes (book-length chapters),[75] providing an accurate regional inventory of the areal extent of glaciers on the planet, with different chapters focusing on different geographic areas. Additionally, Chapter 1386-A[76] focuses on changes in the cryosphere, and trends related to global warming.[2] Prior to that, William O. Field compiled a NH atlas of mountain glaciers.[77]

The goal of GLIMS is to build and populate a Web-accessible database of glacier data for the approximately 160,000 non-ice sheet glaciers worldwide to produce a globally comprehensive and consistent set of glacier outlines.[70,78] Like the Satellite Image Atlas series, this project is characterized by broad international cooperation. Recently, the global inventory of glacier outlines, called the 'Randolph Glacier Inventory', or RGI 1.0: www.glims.org/RGI, (http://www.glims.org/RGI/randolph.html) was produced as reported.[79] Estimates from different methods that yield long time series indicate steady increases in ice loss from glaciers since about 1985 with a slight decline in the most recent years. The inventories indicate that since the 1990s, several hundred glaciers globally have completely disappeared. Overall, the more complete data indicate that glaciers worldwide have lost mass at an average rate of 226 ± 135 Gt/year (very likely) for the period 1971–2009 while they lost about 275 ± 135 Gt/year (very likely) for the period 1993–2009.[80] For reference, a mass loss of 362 Gt of land ice (to the oceans) causes about 1 mm rise in global sea level.

Greenland Ice Sheet

Mass loss of the Greenland ice sheet has accelerated in the last decade due to increases in ice discharge and surface meltwater runoff.[6,81–83] Enhanced melting has been reported using passive microwave data,[84] Gravity Recovery and Climate Experiment (GRACE) data[81] and laser altimetry data.[85,86] Thinning along the ice sheet margins and some thickening at the higher elevations was previously observed using aircraft altimetry[85] and this has since been confirmed by independent studies using GRACE data[81] and ICESat laser altimetry data.[87] The mass loss estimated using the various techniques has not been very consistent and ranged from −6 to 74 Gt/year over the period 1992–2001 and from 157 to 274 Gt/year over the period 2002–2011. Taking a simple average, the observations indicate a change in mass loss from 34 Gt/year for the earlier period to 215 Gt/year for the latter period.[80]

Increased surface melt has also been measured on the Greenland ice sheet using infrared (IR) data.[19,88–90] These studies have largely been accomplished using individual sensors such as from the AVHRR and MODIS (Figure 5). In addition, AMSR-E and the QuikSCAT scatterometer[20] can provide more information, such as surface and near-surface melt through cloud cover. Melt originating on and near the surface is especially important in the lower parts of the ice sheet where much of the surface water runs off, or percolates through the ice to the bottom and serves as a lubricant that can speed up parts of the ice sheet.[91] Such phenomenon could threaten the stability of the ice sheet but the

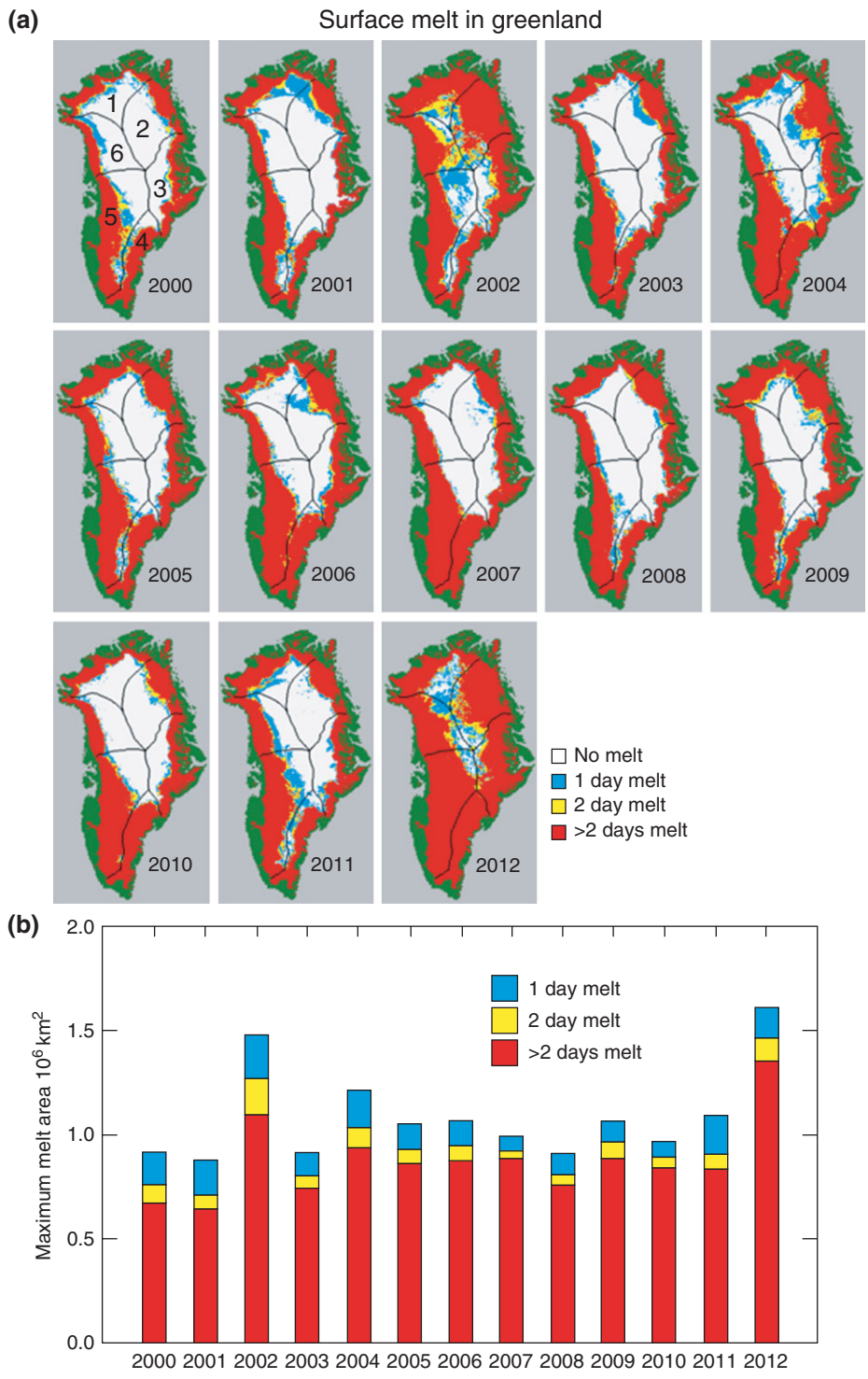

FIGURE 5 | (a) Maps of annual maximum melt extent constructed from moderate-resolution imaging spectroradiometer (MODIS) IST data of the Greenland ice sheet for the study period (March 2000 through August 2012). The nonice sheet covered land surrounding the ice sheet is shown in green. The boundaries of the six major drainage basins of the Greenland ice sheet are superimposed on the maps. (b) Extent of maximum melt in each melt season as derived from the MODIS IST data record; colors relate to those shown in (a). Note the large amount of melt in 2012 that lasted for >2 days. The melt extent in 2002 is also notably large. (Reprinted with permission from Ref 19. Copyright 2007 United States Government as represented by the Administrator of the National Aeronautics and Space Administration)

mechanism is poorly understood and may be driven by melt water supply variability.[92]

Changes in Permafrost

Permafrost, a major component of the terrestrial cryosphere, is ground that remains at or below 0°C for at least two consecutive years (Figure 1). Permafrost occupies about 24% of the land area in the NH. The temperature of permafrost in the Arctic is −10°C or lower in the cold regions and −1°C or lower in the warmer regions while the thickness ranges from ∼1400 m to just a few centimetres.[93] Continuous permafrost is defined as permafrost that is found everywhere beneath the surface (except under some lakes), while discontinuous permafrost is absent from beneath some land areas, and can be sporadic. The active layer, the ground overlying permafrost that thaws in the summer, tends to be thinner in areas of continuous permafrost. Though the active layer can support vegetation, roots typically spread laterally and permafrost is a barrier to rooting depth.

Obtaining quantitative information about permafrost using remotely-sensed data is a very difficult endeavor. For one thing, the active layer obscures the frozen ground below. Also, it is difficult to distinguish from space between seasonally frozen ground and permafrost, though surface clues can help. The remote sensing of permafrost is in its infancy, however, much important research has been accomplished. In this section, we highlight some work to provide the reader with information about the state of the art of the remote sensing of permafrost for climate-change trend studies.

As discussed earlier, many studies have shown convincing observational and modeling evidence for a sustained warming of the Arctic. Surface temperature is the primary climatic factor that governs the existence, spatial distribution, and thermal regime of permafrost.[94] And the well-documented warming of the Arctic is reflected in the observed increases of permafrost temperatures, though snow-cover thickness and other effects also contribute to changes in the permafrost temperature. For example, in Alaska, during the last quarter of the 20th century, permafrost had generally warmed across the state, by ∼3–4°C in the Arctic Coastal Plain, 1–2°C in the Brooks Range, and ∼0.3–1°C south of the Yukon River.[95]

In fact, a general increase in permafrost temperatures is observed during the last several decades not only in Alaska but also in northwest Canada and Siberia[96–100] (Figure 6). When the permafrost temperature increases, this results in a thickening of the active layer, and development of thermokarst which is an irregular land surface of marshy hollows and small hummocks following the thawing of the permafrost.

In Figure 6, changes in the thickness of the active layer, or active-layer thickness (ALT) are shown for nine different areas in the NH.[96] There is quite a bit of variability in ALT and in change in ALT, but there is a general increase in ALT, especially for the Greenland, Russian European North, and the Russian Far East sites.

Permafrost thawing and thermokarst development are associated with improved drainage, i.e., vertical movement of water through the soil, thus leading to changes in the distribution and extent of plant communities. For example, over about the last 15 years, active-layer thickness on the Alaskan North Slope and in the western Canadian Arctic was relatively stable, whereas it increased in the Russian European North, the region north of East Siberia, Chukotka, Svalbard, and Greenland.[96] Intensified shrub growth in the tundra in northern Alaska has resulted from increasing summer temperatures over the last 50 years or so.[102] If shrub growth and height increase on a larger scale, this could reduce surface albedo, increase absorption of solar radiation and be a positive feedback mechanism associated with a warming climate.[103]

Permafrost will start to thaw when its mean-annual temperature increases to above 0°C for more than two consecutive years. Peatlands that are underlain by permafrost emit CH_4 (methane) to the atmosphere, thus permafrost thawing contributes to the release of a significant amount of greenhouse gas emission, primarily CH_4 and carbon dioxide (CO_2) stored in organic frozen soils.[104] CH_4, a potent greenhouse gas, accumulates in subsurface hydrocarbon reservoirs, such as coal beds and natural gas deposits. And CH_4 release has been documented from various locations in the Arctic and sub-Arctic. In the Arctic, permafrost and even glaciers form a 'cryosphere cap' that traps gas leaking from these reservoirs, restricting flow to the atmosphere. The top 3 m of Arctic permafrost contain about 1000 petagrams (Pg) (a petagram is 10^{15} grams, or a billion metric tons) of carbon as organic matter that could be converted to methane,[105] which is a large part of the estimated global atmospheric methane pool. Over 150,000 seeps of CH_4 gas have been mapped in the pan-Arctic through permafrost, resulting from the shrinkage of glaciers, often through active faults, and the Greenland ice sheet.[100] According to some studies, thawing of permafrost along margins of thaw lakes in North Siberia accounts for most of the methane released from lakes.[106]

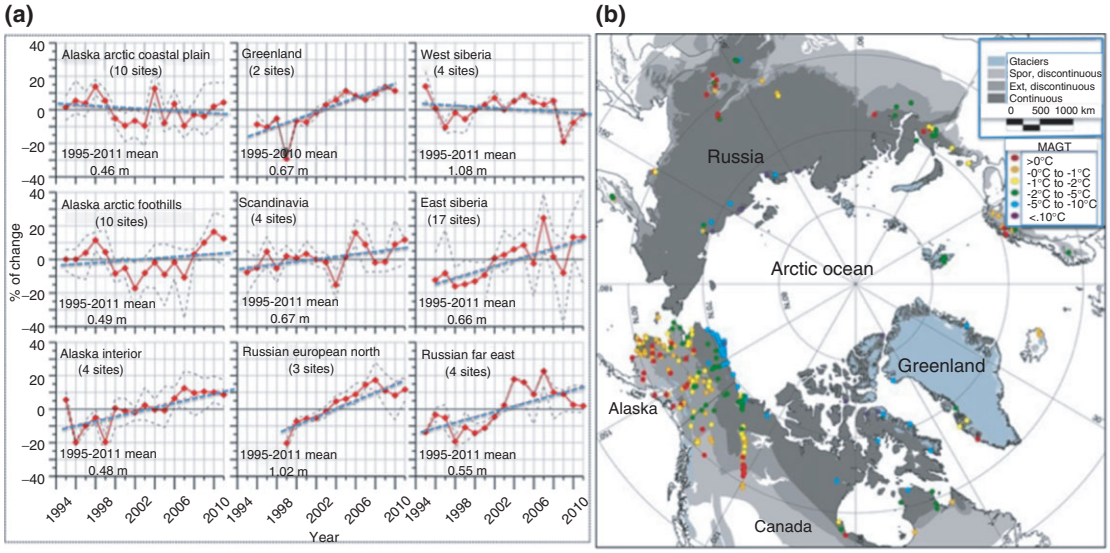

FIGURE 6 | (a) Circum-Arctic view of mean annual ground temperature (MAGT) in permafrost during the International Polar Year (IPY 2007–2009); (a) active-layer change in nine different Arctic regions according to the Circumpolar Active Layer Monitoring (CALM) program. The data are presented as annual percentage deviations from the mean value for the period of observations (indicated in each graph). Solid red lines show mean values. Dashed gray lines represent maximum and minimum values. Thaw depth observations from the end of the thawing season were used. The number of CALM sites within each region varies and is indicated in each graph. (Reprinted with permission from Ref 101. Copyright 2012 John Wiley and Sons; Ref 96. Copyright 2012 The Northern Publisher Salckhard)

CHANGES IN RELATED VARIABLES

Changes in Albedo

Surface albedo is an important component of the climate system because of its role in controlling the amount of heat from the sun that is absorbed by the surface. The albedo of ice and snow is among the highest on the surface of the Earth but the value varies depending on surface type and can cover a large range. For snow-covered surfaces, albedo is affected by many factors including the grain size, age, thickness, and the liquid content of the snow.[107,108] For bare ice, albedo is also affected by presence of surface water and ice thickness. The surface albedo in the Arctic thus changes during the onset of melt when liquid water covers individual snow grains and when diurnal melt and refreeze occurs, causing the snow grain size to increase. In the summer, significant changes also occur on sea ice because of melt effects and the formation of melt ponds which can be as extensive as 30%.[109] In autumn, the albedo again changes during the transition period when the snow cover starts to accumulate.

The mean albedo of the Arctic region has declined considerably because of the aforementioned shrinkage in the sea ice and snow cover. Such decline has been exacerbated by increases in the amount of soot particles that are transported to the polar regions.[110] Furthermore, the onset of melt has been observed to be occurring earlier during the spring period.[111,112] Quantitative estimates of the changes in albedo in the Arctic region have been done using satellite AVHRR data.[113,114] Uncertainties can be relatively high because the time series data are from many AVHRR sensors that are not intercalibrated and the cloud masking is not perfect. However, intercalibration can be improved through the use of reference targets, like Greenland or Antarctica, at certain times of the year when they have predictable albedo values.

To illustrate how albedo has been changing during the satellite era, color-coded averages of narrowband albedo for the years 1982–1996 and from 1997 to 2011 are presented in Figure 7(a) and (b), respectively. The values are actually normalized radiances at 0.6 μm, expressed in units of albedo using as a known reference albedo in Greenland and open ocean. Averages are very similar for the two periods with the exception of the sea ice cover where large changes from the first to second period have been observed. A color-coded difference map, presented in 7c, provides a more quantitative evaluation of the changes in various parts of the Arctic and it is apparent that the big negative changes occurred in the sea ice edge regions in the summer where rapid decline of sea ice has been occurring. For comparison, Figure 7(d) is the result of trend analysis for each pixel and it is apparent that the trends for the entire period are very similar to the difference of mean albedo for the first and second period.

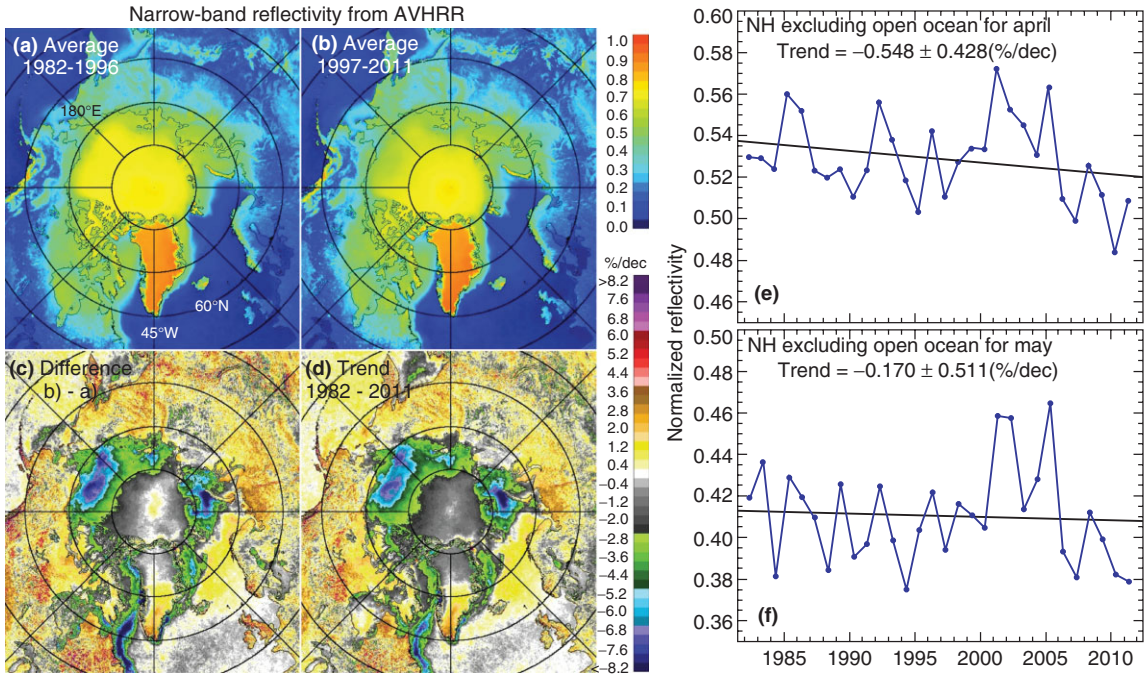

FIGURE 7 | Multiyear averages of advanced very high resolution radiometer (AVHRR) narrow-band albedo (normalized to range from 0 to 1) from (a) 1982 to 1996 and (b) 1997 to 2012; (c) difference of (a) and (b). (d) Color-coded trend map for the period 1982–2012. Average monthly albedo over land and sea ice from 1982 to 2012 for (e) April and (f) May.

To assess how the Arctic albedo has been changing during spring, the average monthly albedo for April and May in the NH are presented in Figures 7(e) and (f), respectively. Trend analysis shows trends of -0.74 ± 0.42%/decade (likely, representing 66% confidence level) in April and -0.33 ± 0.49%/decade (likely) in May. The negative trends are consistent with observed changes in surface characteristics and the negative trends in the spring snow-cover and sea ice extent. The errors indicated are again the statistical errors of the trends which are relatively large mainly on account of large interannual variability. There are also large systematic errors associated with imperfect cloud masking and intercalibration of the different sensors that are difficult to quantify but the year to year variations of such errors are not considered significant and likely would not affect the trend.

Changes in Cloud Cover

The important role of clouds on the Arctic climate, especially in association with feedback effects, has been reported in many studies.[2,114–116] The decline in the cloud cover has been used as one of the reasons for the dramatic decline in the ice cover in the summer of 2007[117] The same phenomenon may also explain unusually high average SST values in the Beaufort/Chukchi Sea region in 2007. Clouds can cause a cooling or a warming of the Earth's surface depending on cloud type. High clouds tend to cause a cooling effect since they shield the Earth's surface from solar radiation by reflecting the radiation back to outer space. Low and thick clouds usually have a warming effect since they absorb and reemit long wave radiation back to the surface. On the other hand, cloud-free conditions make the ice-albedo feedback phenomenon operate more effectively in light of the rapidly retreating sea ice cover in the summer.

Interannual changes and trends in the Arctic cloud cover are largely unknown because of the lack of reliable long-term cloud data. To gain insight into how Arctic clouds have been changing, we present in Figure 8 plots of time series of monthly anomaly cloud fraction data as derived from AVHRR for the period from August 1981 to November 2012. Monthly averaged cloud fraction data (not shown) in the Arctic (>60 °N) show large seasonal and interannual variability (not shown), but persistently high percentages ranging from 65% to 85%. Interannual changes are more apparent in the monthly anomaly plots and are shown separately for the ice covered and ice free regions of the Arctic in Figures 8(a) and (b), respectively. The monthly variability is high while the trends are relatively weak over the August 1981–November 2012 period and are shown to be -1.45 ± 0.15%/decade

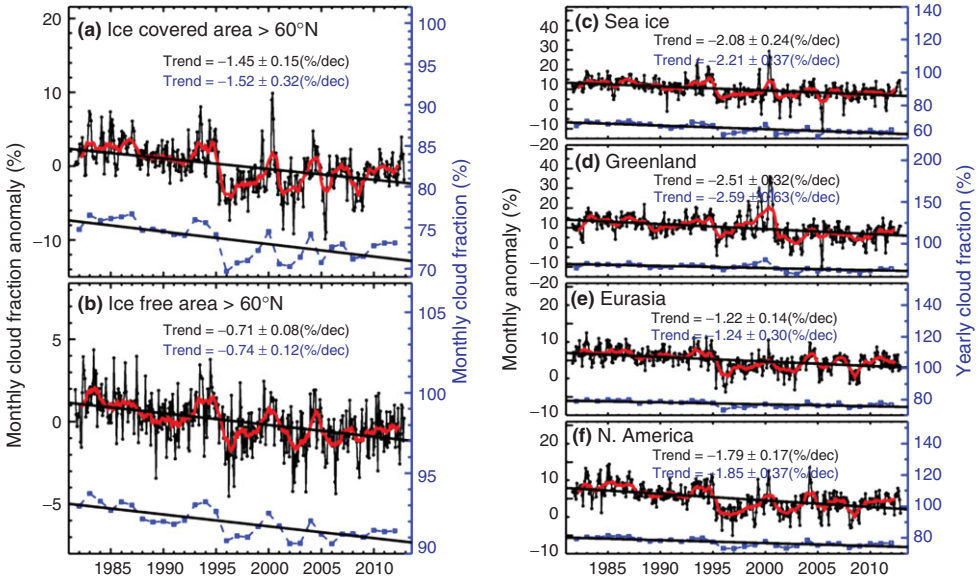

FIGURE 8 | (a) Monthly anomalies of cloud fraction in the Arctic (>60°N) over (a) ice covered; (b) ice free ocean areas; (c) sea ice; (d) Greenland; (e) Eurasia; and (f) North America.

(likely) and -0.71 ± 0.08%/decade (likely) for ice covered and ice free regions, respectively. Similar plots are presented over different regions and regression analysis yielded the likely trends in cloud fraction of -2.08 ± 0.24%/decade over sea ice, -2.51 ± 0.32%/decade over Greenland, -1.22 ± 0.14%/decade over Eurasia, and -1.79 ± 0.17%/decade over North America. The trends are consistently negative with the most negative over Greenland. Yearly averages (of August of one year to July the following year) are also provided showing similar distributions as the 12-month running averages (in red) of the monthly anomalies and actual cloud fractions. The errors in the trends, as indicated, are statistical errors and are shown to be significantly lower than the trends. Trend analysis was also done using yearly averages and the results are consistent with those derived from the monthly anomalies but with larger errors.

The launch of MODIS, CloudSat, and Cloud Aerosol Lidar and Infrared Pathfinder Satellite Observation (CALIPSO) all in the A-train, has made it possible to obtain almost full characterization of clouds including estimates of the height, thickness, optical depth, though type of cloud is an even more challenging problem. The set of near-simultaneous data provides a very promising capability to perform cloud cover studies but more work needs to be done to obtain consistency in the estimates from among these three sensors[118] MODIS provides more accurate cloud data than AVHRR but the current time series is too short for meaningful trend analysis.

Changes in Atmospheric Circulation

The Arctic Oscillation (AO), often referred to as Northern Annular Mode (NAM), has been regarded as among the most dominant modes in the NH, affecting atmospheric circulation and climate in the Arctic. Its direct impacts on the sea ice cover and wind circulation patterns have been evaluated using AO indices as presented for the entire year on a monthly basis in Figure 9(a) and for the winter period in Figure 9(b). The plots show that the indices for both monthly and for the winter season are mainly positive since 1988 although there are years (e.g., 2010) when they become strongly negative. It has been previously reported that negative AO indices are associated with extensive ice cover while positive indices would correspond to a reduced sea ice cover.[119] However, the indices have become nearly neutral in the recent decade while the sea ice cover continued to decline. Recent analysis using data from 1979 to 2012 yielded very poor correlation of AO indices in winter with the sea ice extent and area for both perennial and multiyear ice (see Figure 3(f)).[32] It is also apparent that there is no connection of the large negative anomaly of the AO index in 2010 with the observed changes in the sea ice cover. The influence of AO on the recent changes in the Arctic is currently not well understood and some studies even suggest that there has been a radical shift of atmospheric circulation that is leading to a rapid change in the Arctic climate system.[120] An amplification mechanism that involves increased interaction between the Arctic climate and sub-Arctic weather has also been proposed as a key factor

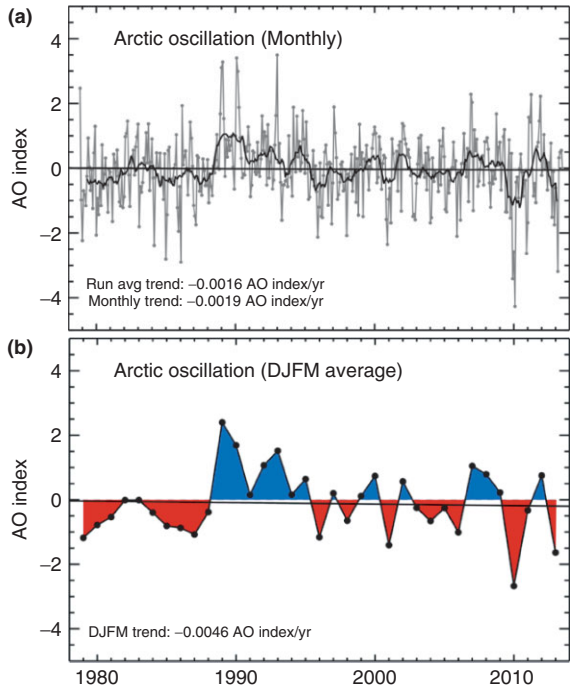

FIGURE 9 | Monthly anomalies of the Arctic Oscillation (AO) indices for (a) each month and (b) each winter (December, January, February, and March) the period 1979–2012.

associated with observed changes in the Arctic.[121] The occurrence of more leads in winter associated with changing atmospheric circulation could also increase the temperature of the mixed layer causing more ice to melt. There is thus a need for a more in-depth understanding of the basic mechanisms associated with feedbacks and the interaction of observed changes in the Arctic with the Arctic climate system.

FUTURE OBSERVATIONAL AND MODELING REQUIREMENTS

Observational Requirements

With the Arctic changing so rapidly, it is important to gain insights into the key factors that may be contributing to the changes. The observational needs are many and include detailed and accurate measurements of ocean, atmospheric and ice parameters. The observed changes are the result of a complex interaction of these various parameters. For example, to gain an improved understanding about the rapidly changing perennial and multiyear sea-ice cover, we need to know not just how the extent is changing but also how the thickness of the ice and its snow cover are changing. We also need measurements of ocean circulation, temperature and salinity to assess how the ice is affected by the underlying water and of atmospheric wind and temperature to quantify the influence of the atmosphere on the ice. The most dependable measurements on thickness of sea ice have been the very sparse historical data provided by submarine upward-looking sonars. With the advent of satellite lidar and Doppler radar altimetry, we can have sea ice thickness at a good spatial and temporal resolution. The technique measures the thickness of the freeboard layer (the layer above the water line) and assumes knowledge of the density of the ice.[122] One of the requirements is thus an ability to obtain snow-cover thickness through satellite or other observations. Some radar systems flown on board aircraft have shown good potential but space-based systems also need to be developed. In this regard, ability to quantify the amount and rate of solid precipitation would also be desirable. Such data would be useful not only for sea ice studies but also for studies of other cryospheric phenomena such as accumulation rates over the ice sheets.

Ability to obtain pan-Arctic snow-cover information from satellite visible channel data is also a problem during winter when much of the Arctic region is in darkness and/or is obscured by clouds. Passive microwave data have been very useful in this regard but the resolution of current systems is relatively coarse and for many applications high resolution data are needed. Such data would also be useful for studies of mountain glaciers and permafrost during the winter and during darkness.

Quantitative observations of the amount of methane that is released from permafrost and other regions would also be desirable. As the Arctic continues to warm, the amount of methane released will increase and the impact of methane on global warming is likely to become a serious problem. An ability to monitor atmospheric methane in permafrost regions using space-based sensors could provide much of the required information.

Modeling Requirements

The future state of the Arctic climate has been of intense interest because of the observation of large changes in the region during the last few decades. To improve our understanding of the significance of the observed changes, there is a need for a numerical model that incorporates the physics of the system and is able to simulate the observed variability and trends of the various parameters in the system. Such a model could then be used to do sensitivity studies to test the influence of various parameters, including greenhouse gases, on the climate system. It can also

be used to extend the observed trends and make projections for the future. Many such models have been developed over the years with different degrees of success.[44,101,123] Some discrepancies are expected because of the chaotic nature of the system and the difficulty to take into account the physics of short-term changes within the system. A key problem is that most of the models are designed to do long-term projections as opposed to short-term projections. Although long-term projections are also important, with the observed changes occurring at a relatively fast phase, it is important to be able to simulate the short-term behavior of the system as well. A modeling requirement would thus be the development of a new breed of models that is able to make accurate predictions of the decadal changes of the variables within the system. It is also important that the credibility of the models is validated through comparative analysis with observed data. Such models would be invaluable especially to policy makers who need to know the severity of the change, the risks and potential impacts on a short-term basis.

CONCLUSION

We have provided a general assessment of the current state of the Arctic climate as derived from historical satellite and *in situ* data. Warming in the Arctic has been amplified, as expected from ice-albedo feedback and other effects and as predicted by models, with the rate of warming increasing from 0.2°C/decade globally to about 0.6°C/decade in the Arctic (>64°N) during the period 1981 to 2012. The data also show that the rate of increase in surface temperature has been accelerating. Such increases in the rate of warming are manifested in all components of the cryosphere. The annual sea ice extent has been declining at the rate of 3.8%/decade while the perennial ice extent (representing the thick component) is declining at a much greater rate of 11.5%/decade. The NH spring snow cover has also been declining at a rate of 2.12%/decade since 1967. The Greenland ice sheet has been losing mass at the rate of 34 Gt/year (sea level equivalence of 0.09 mm/year) during the 1992 to 2001 period but an acceleration to 215 Gt/year is apparent for the period 2002 to 2011 using new instrumentations (e.g., GRACE). The glaciers worldwide which have been losing mass at the rate of 226 Gt per year during the period 1971 to 2009 have been losing more mass in more recent years (1992 to 2009) at the rate of 275 Gt per year. Significant changes in permafrost have also been observed, with many parts of the NH such as Alaska, northwest Canada, and Siberia reporting increased permafrost temperatures and a thickening of the active layer that overlies permafrost. For example, near the end of the 20th Century, permafrost temperatures in northern Alaska had increased by up to ~3–4°C on the Arctic Coastal Plain. Related variables are also observed to be changing. Consistent with the reported decline of the sea ice and snow cover, the average surface albedo during spring and summer is also declining.

ACKNOWLEDGMENTS

The authors would like to acknowledge the work of Nicolo E. DiGirolamo of SSAI and NASA/GSFC, for skilled programming and help to develop figures for this manuscript. Also, the excellent programming and analysis support for this project from Robert Gersten of RSI and Larry Stock of SGT is greatly appreciated.

REFERENCES

1. Holland MM, Bitz CM. Polar amplification of climate change in coupled models. *Clim Dyn* 2003, 21:221–232. doi: 10.1007/s00382-003-0332-6.
2. Kellogg WW. Feedback mechanism in the climate system affecting future levels of carbon dioxide. *J Geophys Res* 1983, 88C2:1263–1270.
3. Hall DK, Robinson DA. Global snow cover. In: Williams RS Jr, Ferrigno JG, eds. *Satellite Image Atlas of Glaciers of the World, State of the Earth's Cryosphere at the Beginning of the 21st Century*, USGS Professional Paper 1386-A. 2012, A313–A344.
4. Kaser G, Cogley JG, Dyurgerov MB, Meier MF, Ohmura A. Mass balance of glaciers and ice caps: consensus estimate for 1961–2004. *Geophys Res Lett* 2006, 33:L19501. doi: 10.1029/2006gl027511.
5. Overland JE, Francis JA, Hanna E, Wang M. The recent shift in early summer Arctic atmospheric circulation. *Geophys Res Lett* 2012, 39:L19804. doi: 10.1029/2012GL053268.
6. Rignot E, Velicogna I, van den Broeke MR, Monaghan A, Lenaerts JTM. Acceleration of the contribution of the Greenland and Antarctic Ice Sheets to sea

level rise. *Geophys Res Lett* 2011, 38:L05503. doi: 10.1029/2011GL046583.

7. Romanosky VE, Smith SL, Christiansen HH. Permafrost thermal state in the polar Northern Hemisphere during the International Polar Year 2007–2009: a synthesis. *Permafr Periglac Process* 2010, 21:106–116. doi: 10.1002/ppp.689.
8. Stroeve J, Holland MM, Meier W, Scambos T, Serreze M. Arctic sea ice decline: faster than forecast. *Geophys Res Lett* 2007, 34:L09501. doi: 10.1029.2007GL029703.
9. Hansen J, Ruedy R, Sato M, Lo K. Global surface temperature change. *Rev Geophys* 2010, 48:RG4004. doi: 10.1029/2010RG000345.
10. Jones PD, Wigley TML. Estimation of global temperature trends: what's important and what isn't. *Clim Change* 2010, 100:59–69. doi: 10.1007/s10584-010-9836-3.
11. Karl TR, Trenbert KE. Modern global climate change. *Science* 2003, 302:1719–1723.
12. Rayner NA, Parker DE, Horton EB, Folland CK, Alexander LV, Rowell DP. Global analyses of sea surface temperature, sea ice, and night marine air temperature since the late nineteenth century. *J Geophys Res* 2003, 108D14:4407. doi: 10.1029/2002JD002670.
13. Walsh JE. Climate of the Arctic marine environment. *Ecol Appl* 2008, 18(Supplement):S3–S22.
14. Rigor IG, Colony RL, Martin S. Variations in surface air temperature observations in the Arctic, 1979–97. *J Clim* 2000, 13:896–914.
15. Tung KK, Camp CD. Solar cycle warming at the Earth's surface in NCEP and ERA-40 data: a linear discriminant analysis. *J Geophys Res* 2008, 113:D05114. doi: 10.1029/2007/JD009164.
16. Comiso JC. Warming trends in the Arctic. *J Clim* 2003, 16:3498–3510.
17. Key J, Haefliger M. Arctic ice surface temperature retrieved from AVHRR thermal channels. *J Geophys Res* 1992, 97D5:5855–5893.
18. Hall DK, Comiso JC, DiGirolamo NE, Shuman CA, Key JR, Koenig LS. A satellite-derived climate-quality data record of the clear-sky surface temperature of the Greenland Ice Sheet. *J Clim* 2012, 25:4785–4798. doi: 10.1175/JCLI-D-11-00365.1.
19. Hall DK, Comiso JC, DiGirolamo NE, Shuman CA, Box JE, Koenig LS. Variability and trends in the ice surface temperature and surface melt extent of the Greenland ice sheet from MODIS. *Geophys Res Lett* 2013, 40:2114–2120. doi: 10.1002/grl.50240.
20. Nghiem SVDK, Hall TL, Mote M, Tedesco M, Albert K, Keegan CA, Shuman NEDG, Neumann G. The extreme melt across the Greenland ice surface in 2012. *Geophys Res Lett* 2012, 39:L20502. doi: 10.1029/2012GL053611.
21. Comiso JC. *Polar Oceans from Space*. New York: Springer Publishing; 2010. 10.1007/978-0-387-68300-3
22. Steele M, Ermold W, Zhang J. Arctic Ocean surface warming trends over the past 100 years. *Geophys Res Lett* 2008, 35:L02614. doi: 10.1029/2007GL031651.
23. Holland MM, Bitz CM, Tremblay B, Bailey DA. The role of natural versus forced change in future rapid summer Arctic ice loss. In: DeWeaver ET, Bitz CM, Tremblay LB, eds. *Arctic sea ice decline: observations, projections, mechanisms, and implications*, vol. 180 Geophysical Monograph Series. Washington, D. C.: AGU; 2008, 133–150.
24. Chelton DB, Wentz F. Global microwave satellite observations of sea surface temperature for numerical weather prediction and climate research. *Bull Am Meteorol Soc* 2005, 86(8):1097–1115. doi: 10.1175/BAMS-86-8-1097.
25. Shibata A, Murakami H, Comiso J. Anomalous warming in the Arctic Ocean in the summer of 2007. *J Remote Sens Soc Jpn* 2010, 30:105–113.
26. Gloersen P, Campbell W , Cavalieri D , Comiso J , Parkinson C , Zwally HJ . Arctic and Antarctic Sea Ice, 1978–1987: satellite passive microwave observations and analysis. NASA Special Publication 511. 1992
27. Comiso JC. A rapidly declining perennial sea ice cover in the Arctic. *Geophys Res Lett* 2002, 29:1956. doi: 10.1029/2002GL015650.
28. Cavalieri DJ, Parkinson CL. Arctic sea ice variability and trends, 1979–2010. *Cryosphere* 2012, 6:881–889. doi: 10.5194/tc-6881-2012.
29. Johannessen OM, Bengtsson L, Miles MW, Kuzmina SI, Semenov VA, Alekseev GV, Ngurnyi AP, Zakharov VF, Bobylev LP, Pettersson LH, et al. Arctic climate change: observed and modeled temperature and sea ice variability. *Tellus* 2004, A56:328–341.
30. Comiso JC, Parkinson CL, Gersten R, Stock L. Accelerated decline in the Arctic sea ice cover. *Geophys Res Lett* 2008, 35:L01703. doi: 10.1029/2007GL031972.
31. Simonds I, Rudeva I. The great Arctic cyclone of August 2012. *Geophys Res Lett* 2012, 39:L23709. doi: 10.1029/2012GL054259.
32. Parkinson CL, Comiso JC. On the 2012 record low Arctic sea ice c over: combined impact of preconditioning and an August storm. *Geophys Res Lett* 2013, 40:1–6. doi: 10.1002/grl.50349.
33. Zhang JR, Lindsay AS, Steele M. The impact of an intense summer cylone on 2012 Arctic sea ice retreat. *Geophys Res Lett* 2013, 40(4):720–726. doi: 10.1002/grl.50190.
34. Cavalieri DJ, Gloersen P, Campbell WJ. Determination of sea ice parameters with the Nimbus 7 SMMR. *J Geophys Res* 1984, 89:5355–5369.
35. Svendsen EK, Kloster K, Farrelly B, Johannessen OM, Johhannessen JA, Campbell WJ, Gloersen P,

Cavalieri DJ, Matzler C. Norwegian remote sensing experiment: evaluation of the Nimbus 7 Scanning Multichannel Microwave Radiometer. *J Geophys Res* 1983, 88C5:2781–2792.

36. Swift CT, Fedor LS, Ramseier RO. An algorithm to measure sea ice concentration with microwave radiometers. *J Geophys Res* 1985, 90C1:1087–1099.
37. Comiso JC. Characteristics of winter sea ice from satellite multispectral microwave observations. *J Geophys Res* 1986, 91C1:975–994.
38. Steffen K, Cavalieri DJ, Comiso JC, St Germain K, Gloersen P, Key J, Rubinstein I. The estimation of geophysical parameters using Passive Microwave Algorithms. In: Carsey F, ed. *Microwave Remote Sensing of Sea Ice*, Chapter 10. Washington, D.C.: American Geophysical Union; 1992, 201–231.
39. Comiso JC, Cavalieri DJ, Markus T. Sea ice concentration, ice temperature, and snow depth, using AMSR-E data. *IEEE TGRS* 2003, 41:243–252.
40. Comiso JC, Parkinson CL. Arctic sea ice parameters from AMSR-E using two techniques, and comparisons with sea ice from SSM/I. *J Geophys Res* 2008, 113:C02S05. doi: 10.1029/2007JC004255.
41. Parkinson CL, Cavalieri DJ. Arctic sea ice variability and trends, 1970–2006. *J Geophys Res* 2008, 113:C07003. doi: 10.1029/2007JC004558.
42. Comiso JC, Nishio F. Trends in the sea ice cover using enhanced and compatible AMSR-E, SSM/I, and SMMR data. *J Geophys Res* 2008, 113:C02S07. doi: 10.1029/2007JC004257.
43. Kinnard C, Zdanowicz CM, Fisher DA, Isaksson E, De Vernal A, Thompson LG. Reconstructed changes in Arctic sea ice over the past 1,450 years. *Nature* 2011, 479:509–512.
44. Wang M, Overland JE. A sea ice free summer Arctic within 30 years-an update from CMIP5 models. *Geophys Res Lett* 2012, 39(18):L18501. doi: 10.1029/2012GL052868.
45. Comiso JC. Large decadal decline in the Arctic multiyear ice cover. *J Clim* 2012, 25:1176–1193. doi: 10.1175/JCLI-D-11-00113.1.
46. Rothrock DA, Yu Y, Maykut GA. Thinning of the Arctic sea-ice cover. *Geophys Res Lett* 1999, 26:3469–3472.
47. Wadhams P, Davis NR. Evidence of thinning of the Arctic ice cover north of Greenland. *Nature* 2000, 345:795–797.
48. Kwok R, Rothrock D. Decline in Arctic sea ice thickness from submarine and ICESat records: 1958–2008. *Geophys Res Lett* 2009, 36:L15501. doi: 10.1029/2009GL039035.
49. Walsh JE, Chapman WL. 20th century sea-ice variations from observational data. *Ann Glaciol* 2001, 33:444–448.
50. Groisman PY, Karl TR, Knight RW. Observed impact of snow cover on the heat balance and the rise of continental spring temperatures. *Science* 1994, 263:198–200. doi: 10.1126/science.263.5144.198.
51. Déry SJ, Brown RD. Recent Northern Hemisphere snow cover extent trends and implications for the snow-albedo-feedback. *Geophys Res Lett* 2007, 34:L22504. doi: 10.1029/2007GL031474.
52. Matson M, Wiesnet DR. New data base for climate studies. *Nature* 1981, 289:451–456.
53. Ramsay BH. The interactive multisensor snow and ice mapping system. *Hydrol Process* 1998, 12:1537–1546.
54. Helfrich S, McNamara D, Ramsay B, Baldwin T, Kasheta T. Enhancements to, and forthcoming developments in the Interactive Multisensor Snow and Ice Mapping System (IMS). *Hydrol Process* 2007, 21:1576–1586. doi: 10.1002/hyp.6720.
55. Robinson DA, Dewey K, Heim R. Global snow cover monitoring: an update. *Bull Am Meteorol Soc* 1993, 74:1689–1696. doi: 10.1175/1520-0477.
56. Riggs GA, Hall DK, Salomonson VV. MODIS snow products user guide; 2006. Available at: http://modis-snow-ice.gsfc.nasa.gov/sugkc2.html
57. Hall DK, Riggs GA. Accuracy assessment of the MODIS snow-cover products. *Hydrol Process* 2007, 21:1534–1547. doi: 10.1002/hyp.6715.
58. Brown RD, Robinson DA. Northern Hemisphere spring snow cover variability and change over 1922–2010 including an assessment of uncertainty. *Cryosphere* 2011, 5:219–229. doi: 10.519/tc-5-219-2011.
59. Derksen C, Brown R. Spring snow cover extent reductions in the 2008–2012 period exceeding climate model projections. *Geophys Res Lett* 2012, 39:L19504. doi: 10.1029/2012GL053387.
60. Foster JL. The significance of the data of snow disappearance on the Arctic Tundra as a possible indicator of climatic change. *Arctic Alpine Res* 1989, 21:60–70.
61. Foster JL, Winchester JW, Dutton EG. The data of snow disappearance on the Arctic tundra as determined from satellite meteorological station and radiometric in situ observations. *IEEE Trans Geosci Remote Sens* 1992, 30:793–798.
62. Brown R, Braaten R. Spatial and temporal variability of Canadian monthly snow depths, 1946–1995. *Atmos Ocean* 1998, 36:37–54. doi: 10.1080/07055900.1998.9649605.
63. Frei A, Robinson DA, Hughes MG. North American snow extent: 1900–1994. *Int J Climatol* 1999, 19:1517–1534.
64. Stone RS, Dutton EG, Harris JM, Longenecker D. Earlier spring snowmelt in northern Alaska as an indicator of climate change. *J Geophys Res* 2002, D10:4089. doi: 10.1029/2000JD000286.

65. Choi G, Robinson DA, Kang S. Changing Northern Hemisphere snow seasons. *J Clim* 2010, 23:5305–5310. doi: 10.1175/2010JCLI3644.1.
66. Brown R, Derksen C, Wang L. Assessment of spring snow cover duration variability over northern Canada from satellite datasets. *Remote Sens Environ* 2007, 111:367–381. doi: 10.1016/j.rse.2006.09.035.
67. Pu Z, Xu L, Salomonson VV. MODIS/Terra observed seasonal variations of snow cover over the Tibetan Plateau. *Geophys Res Lett* 2007, 34:L06706. doi: 10.1029/2007GL029262.
68. Immerzeel WW, Droogers P, de Jong SM, Bierkens MFP. Large-scale monitoring of snow cover and runoff simulation in Himalayan river basins using remote sensing. *Remote Sens Environ* 2009, 113:40–49.
69. Hall DK, Foster JL, DiGirolamo NE, Riggs GA. Snow cover, snowmelt timing and stream power in the Wind River Range, Wyoming. *Geomorphology* 2012, 137:87–93. doi: 10.1016/j.geomorph.2010.11.011.
70. Raup B, Racoviteanu A, Khalsa SJS, Helm C, Armstrong R, Arnaud Y. The GLIMS geospatial glacier database—a new tool for studying glacier change. *Global Planet Change* 2007, 561–2:101–110.
71. Brown RD, Derksen C. Is Eurasian October snow cover extent increasing? *Environ Res Lett* 2013, 8(2):024006. doi: 10.1088/1748-9326/8/2/024006.
72. Dyurgerov MB, Meier MF. Glacier mass changes and their effect on the Earth system. In: Williams RS Jr, Ferrigno JG, eds, USGS Professional Paper 1386-A. *Satellite Image Atlas of Glaciers, State of the Earth's Cryosphere at the Beginning of the 21st Century*. Professional Paper 1286-A, 2012, A192–A223.
73. Radic V, Hock R. Regionally differentiated contribution of mountain glaciers and ice caps to future sea-level rise. *Nat Geosci* 2011, 4:91–94. doi: 10.1038/nge01052.
74. Paul F, Kaab A, Haeberli W. Recent glacier changes in the Alps observed by satellite—consequences for future monitoring strategies. *Global Planet Change* 2007, 56:111–112.
75. Williams RS Jr, Ferrigno JG. Satellite Image Atlas of Glaciers of the World, USGS Fact Sheet 2005–3056, 2005, (Revised in 2011), 2 p. Available at: http://pubs.usgs.gov/fs/2005/3056.
76. Williams, R.S., Jr. and J.G. Ferrigno. Glaciers, global snow cover, floating ice, and permafrost and periglacial environments *Satellite Image Atlas of Glaciers of the World—State of the Earth's Cryosphere at the Beginning of the 21st Century*, USGS Professional Paper 1386-A, 2012, 546 p.
77. Field WO. *Mountain glaciers of the Northern Hemisphere—atlas*. U.S. Army CRREL publication consisting of regional maps; 1975.
78. Kargel JS, Abrams MJ, Bishop MP, Bush A, Hamilton G, Jiskoot H, Kaab A, Kieffer HH, Lee EM, Paul F, et al. Multispectral imaging contributions to global land ice measurements from space. *Remote Sens Environ* 2005, 991–2:187–219.
79. Arendt A, Bolch T, Cogley JG, Gardner A, Hagen JO, Hock R, Kaser G, Pfeffer WT, Moholdt G, Paul F, et al. Randolph Glacier Inventory [v2.0]: A Dataset of Global Glacier Outlines, Global Land Ice Measurements from Space, Boulder, Colorado, USA. Digital Media; 2012.
80. IPCC2013. *Climate change 2013: the physical basis*. New York: Cambridge University Press; 2013.
81. Luthcke SB, Zwally HJ, Abdalati W, Rowlands DD, Ray RD, Nerem RS, Lemoine FG, McCarthy JJ, Chinn DS. Recent Greenland ice mass loss by drainage system from satellite gravity observations. *Science* 2006, 314:1286–1289.
82. van den Broeke MJ, Bamber J, Ettema J, Rignot E, Schrama E, van den Berg WJ, van Meijgaard E, Velicogna I, Wouters B. Partitioning recent Greenland mass loss. *Science* 2009, 326:984–986. doi: 10.1126/science.1178176.
83. Velicogna I. Increasing rates of ice mass loss from the Greenland and Antarctic ice sheets revealed by GRACE. *Geophys Res Lett* 2009, 36:L19503. doi: 10.1029/2009GL040222.
84. Tedesco M. Snowmelt detection over the Greenland Ice Sheet from SSM/I brightness temperature daily variations. *Geophys Res Lett* 2007, 34:L02504. doi: 10.1029/2006GL028466.
85. Krabill W, Abdalati W, Frederick E, Manizade S, Martin C, Sontag J, Swift R, Thomas R, Wright W, Yungel J. Greenland ice sheet: High-elevation balance and peripheral thinning. *Science* 2000, 289:428–430.
86. Zwally HJ, Li J, Brenner AC, Beckley M, Cornejo HG, DiMarzio J, Giovinetto MB, Neumann TA, Robbins J, Saba JL, et al. Greenland ice sheet mass balance: distribution of increased mass loss with climate warming: 2003–07 versus 1992–2002. *J Glaciol* 2011, 57:88–102.
87. Zwally HJ, Giovinetto MB, Li J, Cornejo HG, Beckley MA, Brenner AC, Saba JL, Yi D. Mass changes of the Greenland and Antarctic ice sheets and shelves and contributions to sea level rise: 1992–2002. *J Glaciol* 2005, 51:509–527.
88. Wang X, Key J. Recent trends in Arctic surface, cloud, and radiation properties from space. *Science* 2003, 299:1725–1728.
89. Wang X, Key J. Arctic surface, cloud, and radiation properties based on the AVHRR Polar Pathfinder data set. Part II: recent trends. *J Climatol* 2005, 18:2575–2593.
90. Comiso JC. Arctic warming signals from satellite observations. *Weather* 2006, 61:70–76. doi: 10.1256/wea.222.05.
91. Zwally HJ, Abdalati W, Herring T, Larson K, Saba J, Steffen K. Surface melt-induced acceleration of Greenland ice-sheet flow. *Science* 2002, 297:218–222.

92. Shoof C. Ice-sheet acceleration driven by melt supply variability. *Nature* 2010, 468:803–806. doi: 10.1038/nature09618.

93. Heginbottom J, Brown J, Humlum O, Svensson H. Permafrost and periglacial environments. In: Williams RS Jr, Ferrigno JG, edsUSGS Professional Paper 1386-A. *Satellite Image Atlas of Glaciers, State of the Earth's Cryosphere at the Beginning of the 21st Century*. 2012, A425–A496.

94. Hachem S, Duguay CR, Allard M. Comparison of MODIS-derived land surface temperatures with ground surface and air temperature measurements in continuous permafrost terrain. *Cryosphere* 2012, 6:51–69. doi: 10.5194/tc-6-51-2012.

95. Osterkamp TE, Jorgenson MT, Schuur EAG, Shur YL, Kanevskiy MZ, Vogel JG, Tumskoy VE. Physical and ecological changes associated with warming permafrost and thermokarst in Interior Alaska. *Permafr Periglac Process* 2009, 20:235–256. doi: 10.1002/ppp.656.

96. Romanovsky VE, Smith SL, Christiansen HH, Shiklomanov NI, Streletskiy DA, Drozdov DS, Oberman NG, Kholodov AL, Marchenko SS. The Arctic Report Card: Permafrost; 2012. Available at: http://www.arctic.noaa.gov/reportcard/permafrost.html.

97. Osterkamp TE, Jorgenson JC. Warming of permafrost in the Arctic National Wildlife Refuge, Alaska. *Permafr Periglac Process* 2006, 17:65–69. doi: 10.1002/ppp.538.

98. Nguyem T-N, Burn CR, King DJ, Smith SL. Estimating the extent of near-surface permafrost using remote sensing, Mackenzie Delta, Northwest Territories. *Permafr Periglac Process* 2009, 20:141–153.

99. Westermann S, Langer M, Boike J. Spatial and temporal variations of summer surface temperatures of high-arctic tundra on Svalbard—implications for MODIS LST based permafrost monitoring. *Remote Sens Environ* 2011, 115:908–922. doi: 10.1016/j.rse.2010.11.018.

100. Woo MK, Mollinga M, Smith SL. Climate warming and active layer thaw in the boreal and tundra environments of the Mackenzie Valley. *Can J Earth Sci* 2007, 44:737–43.

101. Shiklomanov NI, Streletskiy DA, Nelson FE. Northern Hemisphere component of the global Circumpolar Active Layer Monitoring (CALM) Program. In: Hinkel KM, ed. *Proceedings of the 10th International Conference on Permafrost*, vol. 1. Salekhard: The Northern Publisher Salekhard; 2012, 377–382.

102. Sturm M, Racine C, Tape K. Increasing shrub abundance in the Arctic. *Nature* 2001, 41:546–547.

103. Christensen TR, Johansson T, Åkerman HJ, Mastepanov M, Malmer N, Friborg T, Crill P, Svensson BH. Thawing sub-arctic permafrost: effects on vegetation and methane emissions. *Geophys Res Lett* 2004, 31:L40501. doi: 10.1029/2003GL018680.

104. Kerr RA. Arctic armageddon needs more science, less hype. *Science* 2010, 329:620–621. doi: 10.1126/science.329.5992.620.

105. Walter-Anthony KM, Anthony P, Grosse G, Chanton J. Geologic methane seeps along boundaries of Arctic permafrost thaw and melting glaciers. *Nat Geosci* 2012, 5:419–426. doi: 10.1038/NGEO1480.

106. Walter KM, Zimov SA, Chanton JP, Verbyla D, Chapin FS III. Methane bubbling from Siberian thaw lakes as a positive feedback to climate warming. *Nature* 2006, 443:71–75. doi: 10.1038/nature05040.

107. Allison I, Brandt RE, Warren SG. East Antarctic sea ice: albedo, thickness distribution and snow cover. *J Geophys Res* 1993, 98C7:12,417–12,429.

108. Warren S. Optical properties of snow. *Rev Geophys Space Phys* 1982, 20:67–89.

109. Perovich DK, Grenfell TC, Light B, Hobbs PV. Seasonal evolution of the albedo of multiyear Arctic sea ice. *J Geophys Res* 2002, 107C10:8044. doi: 10.1029/2000JC000438.

110. Kim Y, Hatsushika H, Muskett RR, Yamazaki K. Possible effect of boreal wildfire soot on Arctic sea ice and Alaska glaciers. *Atmos Env* 2005, 39:3513–3520. doi: 10.1016/j.atmosenv.2005.02.050.

111. Markus T, Stroeve JC, Miller J. Recent changes in Arctic sea ice melt onset, freezeup, and melt season length. *J Geophys Res* 2009, 114:CV12024. doi: 10.1029/2009JC005436.

112. Wang L, Derksen C, Brown R, Markus T. Recent changes in pan-Arctic melt onset from satellite passive microwave measurements. *Geophys Res Lett* 2013, 40:522–528. doi: 10.1002/grl.50098.

113. Agarwal S, Moon W, Wettlaufer JS. Decadal to seasonal variability of Arctic sea ice albedo. *Geophys Res Lett* 2011, 38:L20504. doi: 10.1029/2011GL049109.

114. Shine KP, Henderson-Sellers A, Barry RG. Albedo-climate feedback: the importance of cloud and cryosphere variability. In: Berger AL, Nicolis C, eds. *New Perspectives in climate modeling*. Amsterdam: Elsevier; 1984, 135–155.

115. Curry JA, Schramm J, Ebert E. Sea ice-albedo climate feedback mechanism. *J Clim* 1995, 8:240–247.

116. Mauritsen T, Graversen RG, Klocke D, Langen PL, Stevens B, Tomassini L. Climate feedback efficiency and synergy. *Clim Dyn* 2013, 41:2539–2554. doi: 10.1007/s00382-013-1808-7.

117. Schweiger AJ, Zhang J, Lindsay RW, Steele M. Did unusually sunny skies help drive the record sea ice minimum of 2007? *Geophys Res Lett* 2008, 35:L10503. doi: 10.1029/2008GL033463.

118. Chan M, Comiso JC. Arctic cloud characteristics as derived from MODIS, CALIPSO, and CloudSat. *J Clim* 2013, 26:3285–3306. doi: jcliD12200204.

119. Rigor IG, Wallace JM, Colony RL. Response of sea ice to the Arctic Oscillation. *J Clim* 2002, 15:2648–2663.

120. Zhang X, Sorteberg A, Zhang J, Gerdes R, Comiso J. Atmospheric circulation signature in recent rapid Arctic climate system change. *Geophys Res Lett* 2008, 35:L22701. doi: 10.1029/2008GL035607.

121. Overland JE, Wood KR, Wang M. Warm Arctic-cold continents: climate impacts of the newly open Arctic Sea. *Polar Res* 2011, 30:15787. doi: 10.3402/polar.v.300.15787.

122. Wadhams P, Tucker W, Krabill W, Swift R, Comiso J, Davis N. The relationship between sea ice freeboard and draft in the Arctic Basin, and implications for ice thickness monitoring. *J Geophys Res* 1992, 97C12:20325–20334.

123. Stroeve JC, Kattsov V, Barrett A, Serreze M, Pavlova T, Holland M, Meier WN. Trends in the Arctic sea ice extent from CMIP5, CMIP3 and observations. *Geophys Res Lett* 2012, 39:L16502. doi: 10.1029/2012GL052676.

